



PERGAMON

Aerosol Science 34 (2003) 169–188

Journal of
Aerosol Science

www.elsevier.com/locate/jaerosci

Hierarchical hybrid Monte-Carlo method for simulation of two-component aerosol nucleation, coagulation and phase segregation

Y. Efendiev^{a,1}, M.R. Zachariah^{b,*}

^a*Institute for Mathematics and its Applications, University of Minnesota, Minneapolis, MN 55455, USA*

^b*Department of Mechanical Engineering and Chemistry, Center for Nano Energetics Research, University of Minnesota, Minneapolis, MN 55455-0111, USA*

Received 16 July 2001

Abstract

In this paper we propose a Monte-Carlo method for the simulation of the simultaneous nucleation, coagulation and phase segregation of an immiscible two-component binary aerosol. The model is intended to qualitatively model our prior studies of the synthesis of mixed metal oxides for which phase segregated domains have been observed in molten nanodroplets. Our new approach generalizes our previous approach (*J. Colloid Interface Sci.*, in press) by incorporating nucleation in addition to coagulation and phase segregation into the method. The nucleation is taken into account using a hierarchy of computational volumes represented in the simulation.

Our attempts to model only the coagulation of heterogeneous aerosols using basic statistics of their internal state (*J. Aerosol Sci.*, to appear; *Chem. Eng. Sci.* 56 (2001) 5763; *J. Nanoparticle Res.*, in press) introduced some limitations. Using Monte-Carlo approaches, on the other hand, we can model the system of heterogeneous aerosols without any a priori assumption.

The Monte-Carlo results show that the growth of the minor phase can be moderated quite dramatically by small changes in system temperature, which effectively serves to change the viscosity of the major phase and therefore the Brownian transport properties of the minor phase.

© 2003 Elsevier Science Ltd. All rights reserved.

Keywords: Monte-Carlo; Two-component aerosol; Nucleation; Coagulation

* Corresponding author. Tel.: +1-612-626-9081; fax: +1-612-625-6069.

E-mail address: mrz@me.umn.edu (M.R. Zachariah).

¹ Present Address: Department of Mathematics, Texas A & M University, College Station, TX 77843, USA.

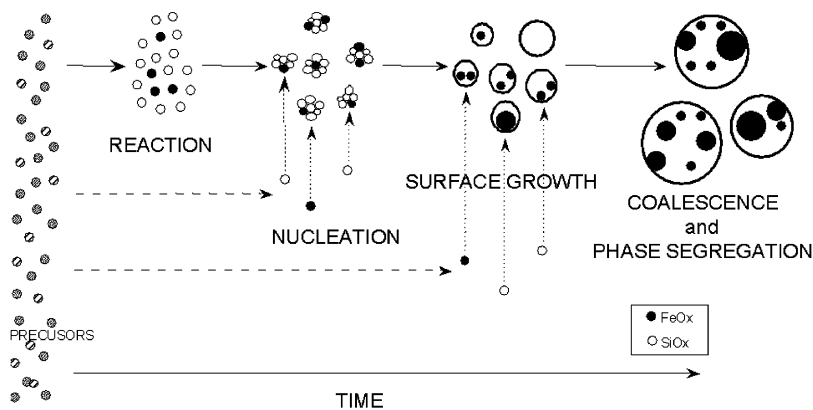


Fig. 1. Schematic description of multi-component aerosol formation.

1. Introduction

The studies employing more than one component aerosol assume that the aerosol is a homogeneous mixture of all the multi-component constituents. On the other hand, there is no a priori reason to assume, this should be the case, and given appropriate thermodynamic and kinetic properties one could expect phase segregated aerosols. In particular, we have observed in several cases that multi-component aerosols can be formed with clearly distinct phases. One of our main goals in this research is to study the evolution of the internal state of such aerosol droplets. For example, we have conducted studies on the formation of binary metal oxide systems with application to removal of heavy metals (Biswas, Yang, & Zachariah, 1998; Biswas & Zachariah, 1997) as well as the formation of materials with novel and interesting properties (Ehrman, Friedlander, & Zachariah, 1998; Ehrman, Aquino-Class, & Zachariah, 1999a; Ehrman, Friedlander, & Zachariah, 1999b).

Our initial success in growing interesting microstructures (Zachariah, Aquino-Class, Shull, & Steel, 1995) indicated that further research into the mechanistic aspects of the growth was warranted.

Based on experimental and computational studies we believe that given that appropriate thermodynamic conditions are present, phase segregation will take place on the time scale of the formation and growth process if at least the major phase is in a liquid state (McMillin, Biswas, & Zachariah, 1996; Biswas, Wu, Zachariah, & McMillen, 1997; Zachariah, Shull, McMillin, & Biswas, 1996).

A schematic description of formation of multi-component heterogeneous aerosols is shown in Fig. 1. We have grown such aerosols from mixtures of liquid metal oxides and metal/salt mixtures (Ehrman et al., 1999a, b; Ehrman et al., 1998; Zachariah et al., 1995; Biswas et al., 1997) generated from gas-phase precursors injected into a high-temperature flame. For example, to form an iron oxide/silica nanoparticle with phase segregated domains we injected iron carbonyl and hexamethyl disiloxane into a methane–oxygen–nitrogen flame. The iron carbonyl vapors enter the flame region, decompose, and oxidized to form iron oxide vapors. Based on known kinetics we have been able to reasonably match the experimentally determined vapor-phase concentration of Fe_2O_3 with a first-order kinetic process in the presence of excess oxygen. Similarly, the oxidation of hexamethyl disiloxane is described by a first-order process in the presence of excess oxygen (Biswas

et al., 1997). These vapors then nucleate to form the oxide particles. Due to the low vapor pressures of the resultant oxides, classical descriptions of the nucleation phenomena indicate that there is no thermodynamic barrier to particle formation, and the process of nucleation can be describe by the kinetics of polymerization.

In the course of this paper we shall use the terms minor phase and enclosure interchangeable to refer to the component within each aerosol droplet, and droplet or aerosol when referring to the particles which do not contain the enclosures. Following our previous works we will assume that the growth of the enclosures takes place due to Brownian interception and the droplets undergo free molecule coagulation. The temporal evolution of the nucleation of aerosols and their coagulation is schematically depicted in Fig. 1. Because our experimental studies were all undertaken when both components were in the molten state we have only observed spherical droplets for both the major and minor phase, which also justifies the use of an instantaneous coalescence assumption in our model.

In our previous work (Struchtrup, Luskin, & Zachariah, 2001; Efendiev, Luskin, Struchtrup, & Zachariah, 2002) a 2-D sectional model was developed to account for the basic statistics of the enclosures inside each droplet, but did not take into account the formation of new particulate material via nucleation. In addition, the description of the enclosure populations inside a droplet introduces limitations because one, in general, cannot describe the evolution of the basic statistics of particle size distribution without an a priori assumption. More recently we developed a hybrid Monte-Carlo method to describe coagulation and phase separation, but not nucleation. This model extends that work to include nucleation effects (Efendiev & Zachariah, 2002).

Monte-Carlo (MC) methods have the advantage that multi-scale and time phenomena can be simultaneously solved without the requirement of a single unifying governing multi-variate equation. Moreover, additional physical effects can be introduced in Monte-Carlo framework often easily. In the simulation of heterogeneous aerosols Monte-Carlo methods are also attractive to us because they do not require any a priori assumptions about the enclosure distribution in each droplet.

Our approach combines two MC simulations. One simulates the coagulation of the droplets and the other simulates the interaction between the enclosures. The nucleation is taken into account by introducing a hierarchy of computational volumes represented in the simulation. Using the hierarchical structure of our approach one can handle large and small number of particles by adjusting the volume represented in the simulation. This procedure is necessary because of the very large swings in number concentration as a result of the kinetics of monomer generation occurring in such systems.

The Monte-Carlo model developed in the paper is applied to the binary $\text{SiO}_2/\text{Fe}_2\text{O}_3$ system, where SiO_2 is considered the major phase and Fe_2O_3 the minor phase (Ehrman et al., 1999a,b). Observationally (Fig. 2) what we seen when sampling from the flame and imaging with TEM is particles with iron oxide enclosures embedded in silica nanoparticles. Furthermore, we notice that with increasing residence time the enclosures grow in size and decrease in number concentration. Recall that under the conditions of growth both phases are in a liquid state (high-temperature growth) and that thermodynamically both phases are immiscible.

Our goal is to determine the distribution of droplet volumes and the internal state of the droplet as a function of time, and the effect of the nucleation on the internal state of the particles. Using our Monte-Carlo approach we study different characteristics of our system depending on monomer production rate, temperature, etc.

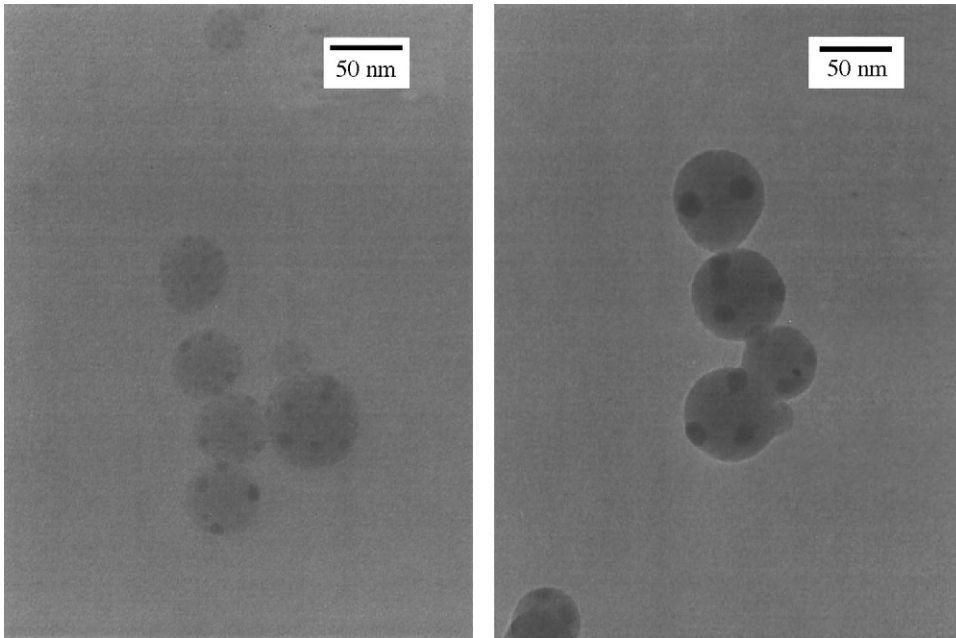


Fig. 2. Evolution of the aerosol (SiO_2) and minor phase (Fe_2O_3) during the growth of $\text{SiO}_2/\text{Fe}_2\text{O}_3$ nanocomposites.

In the next section we address the difficulties associated with modeling the kinematics of heterogeneous particles using macro-scale quantities, such as number density functions. Section 3 is devoted to the description of hierarchical hybrid Monte-Carlo approach and Section 4 its actual implementation. The simulation results are presented in Section 5.

2. Mathematical modeling

The general dynamic equation for a gas to particle conversion in the free-molecule regime is given by Friedlander (2000)

$$\begin{aligned} \frac{\partial N(t, V)}{\partial t} + \frac{\partial(GN(V, t))}{\partial V} - I'(V^*)\delta(V - V^*) \\ = \frac{1}{2} \int_0^V K^F(U, V - U)N(t, U)N(t, V - U) dU - N(t, V) \int_0^\infty K^F(V, U)N(t, U) dU. \end{aligned}$$

The first term on the left-hand side is the rate of change of particle size distribution function in the particle volume V to $V + dV$, the second term on the left-hand side accounts for the effect of condensation at rate G , and the third term on the left-hand side describes the formation of a new particle of critical volume V^* at rate I' . The terms on the right-hand side account for the effect of free-molecule coagulation.

In a heterogeneous droplet of volume V we assume the transport within the droplet is limited to Brownian coagulation. Denoting $n_V(u, t) du$ as the number of enclosures with volume between u

and $u + du$ in the droplet of volume V , Brownian dynamics of the enclosure population obeys the following equation:

$$\frac{dn_V(t, v)}{dt} = \frac{1}{2V} \int_0^v K^D(u, v-u)n_V(t, u)n_V(t, v-u) du - \frac{1}{V} n_V(t, v) \int_0^\infty K^D(v, u)n_V(t, u) du. \quad (1)$$

Note that this equation only describes the coagulation in a droplet and does not include addition of enclosures due to coagulation of enclosures with droplets and coagulation of droplets with other droplets.

For completeness we write the collision kernels for the free-molecule regime coagulation as given by

$$K^F(U, V) = \left(\frac{3}{4\pi}\right)^{1/6} \left(\frac{6kT}{\rho}\right)^{1/2} \left(\frac{1}{U} + \frac{1}{V}\right)^{1/2} (U^{1/3} + V^{1/3})^2 \quad (2)$$

and for the Brownian regime is given by

$$K^D(u, v) = \frac{2kT}{3\mu} (u^{1/3} + v^{1/3}) \left(\frac{1}{u^{1/3}} + \frac{1}{v^{1/3}}\right). \quad (3)$$

Here k denotes Boltzmann's constant, T is the temperature, μ is the viscosity of the medium comprising the droplets and ρ is the density of droplets.

The model describing nucleation and coagulation of heterogeneous aerosols will be given by general dynamic equation for the gas to particle conversion for the droplets, combined with Eq. (1) for the internal dynamics of heterogeneous droplets. In general, solution of this model is quite complicated. Even if one even only considers the coagulation of heterogeneous particles neglecting the nucleation and condensation effects it becomes in general impossible to find the total enclosure distribution. Indeed, in order to find the total enclosure distribution one needs to sum up the individual enclosure distribution over all the droplets. Since the Eq. (1) is nonlinear it is in general impossible to find a single unifying governing equation for the total enclosure distribution. In our previous works (Struchtrup et al., 2001; Efendiev & Zachariah, 2001; Efendiev et al., 2002) we have considered the coagulation of heterogeneous aerosols without taking into account nucleation and condensation effects. The heterogeneous aerosol particles were described using only basic statistics of their internal state in those works. Those approaches required additional assumptions since in general one cannot model the details of the enclosure size distribution without a complete knowledge of particle size distribution. One of the advantages of MC approaches is that we do not require any a priori assumption about the enclosure distribution in each droplet, and the nucleation effects can be incorporated into the MC approach using the concept of hierarchical computational volumes.

3. Hierarchical hybrid Monte-Carlo (MC) method

Monte Carlo simulation is based on the use a finite dimensional subset of the whole system in order to calculate the properties of the system.

A number of Monte-Carlo techniques have been developed for the growth of dispersed systems (Smith & Matsoukas, 1998; Gillespie, 1975; Scott, 1967; Shah, Ramakrishna, & Borwanker, 1977; Tandon & Rosner, 1999; Rosner & Yu, 2001) and they generally fall into two classes. In the first

approach a single event is selected and then the time is advanced by an appropriate increment. In the second approach, for a given time interval a number of successful particle interactions is implemented. In modeling of heterogeneous aerosol we use the second approach for the enclosure interactions. The time is advanced based on the minimum of two time intervals, the coagulation of two droplets or the nucleation of a particle. This time increment then defines how many successful enclosure interactions occurred in each droplet with more than one enclosure.

The finite number of particles used in the simulation introduces some limitations. Because the accuracy of MC is proportional to $1/\sqrt{N}$ (Liffman, 1992) (where N is the number of the particles in the system) one needs to terminate the computation well before there is one particle left. To avoid this problem previous authors (Liffman, 1992; Smith & Matsoukas, 1998) have introduced MC algorithms where the number of the particles are kept constant either by doubling the system when the number of the particles are halved or by replacing a particle after each coagulation. This approach is referred as constant number MC. We employ the former approach in coagulating the droplets.

While the limitations associated with the decrease in the number of particles happens at the later stages of MC simulations, the nucleation event introduces another difficulty associated with the large number of particles. To handle the large number of particles we truncate our system whenever the number of particles becomes larger than some critical number of droplets we would like to simulate. By truncating the system in this way, the characteristic times for coagulation and nucleation are being changed. So that in order to preserve our connection to real time, a new computational volume represented in the simulation has to be calculated.

At each time step of the simulation, two droplets are selected randomly. Based on the volumes of the droplets, V_i and V_j , the total number of the particles in our simulation N_k , and the actual volume represented in the simulation V_{comp} we compute the mean inter-event ΔT time for this coagulation to occur (see also, Smith & Matsoukas, 1998),

$$\Delta T = \frac{2V_{\text{comp}}}{\langle K_{ij}^{\text{F}} \rangle N_k (N_k - 1)}, \quad (4)$$

where $\langle K_{ij}^{\text{F}} \rangle$ is the mean coagulation rate for the system of N_k particles and is given by

$$\langle K_{ij}^{\text{F}} \rangle = \frac{\sum_{i=1}^{N_k} \sum_{j=1, j \neq i}^{N_k} K_{ij}^{\text{F}}}{N_k (N_k - 1)}. \quad (5)$$

At the same time, based on the current actual volume of the simulation, V_{comp} we compute the time interval Δt_n needed for the production of one monomer. In this sense the production rate of monomer is effectively the nucleation event, in the absence of a thermodynamic barrier. In the next section we present an expression for Δt_n for the exponential monomer production rate used in our numerical simulation.

If ΔT is less than or equal to Δt_n we perform the coagulation of the chosen particles based on the chemical composition of the particles (described below). The number of nucleated particles q_k at this time interval is also calculated. Since this number q_k is not necessarily an integer and not larger than unity we introduce the number of the total nucleated particles (monomers) Q_k up to k th time step. At each time step we recalculate Q_k as

$$Q_k = Q_{k-1} + q_k \quad (6)$$

and nucleate $[Q_k]$ particles, where $[Q_k]$ is the integer part of Q_k . Further, Q_k is updated by

$$Q_k = Q_k - [Q_k]. \tag{7}$$

If the nucleation time Δt_n is less than ΔT , then a particle is nucleated. At the same time, the time elapsed from the last particle coagulation should be tracked. After each coagulation of the particles this time is set to zero, and after each nucleation this time is incremented by the nucleation time (monomer generation time) Δt_n .

The coagulation of the chosen particles in our case depends on the composition of the particle. The possibilities are (a) both particles are homogeneous and of the same kind (silica or iron), (b) the particles are homogeneous, but different kinds (one iron and the other silica), (c) one particle is heterogeneous and the other homogeneous, (d) both particles are heterogeneous. In the next section the implementation of this process is described.

After each time increment (no matter if the particles are nucleated or the coagulation of two droplets occurred) we use the elapsed time $\min(\Delta T, \Delta t_n)$ to compute the number of successful enclosure interactions. This restriction on the time step is the primary limitation in the computational speed of the simulation method.

In an analogous manner to that of the droplets we also define the mean inter-event time for the enclosures in a droplet of volume V as

$$\Delta t = \frac{2V}{\sum_{i=1}^{n-1} \sum_{j=1, j \neq i}^{n-1} K_{ij}^D}, \tag{8}$$

where n is the number of the enclosures, and n/V is their number density. From here the number of successful enclosure interactions inside the droplet during the time interval ΔT is given by the integer k which satisfies

$$\sum_{i=1}^k \frac{2V}{\langle K_{ij}^D \rangle (n-i)(n-i-1)} \leq \Delta T \leq \sum_{i=1}^{k+1} \frac{2V}{\langle K_{ij}^D \rangle (n-i)(n-i-1)}. \tag{9}$$

On the left-hand side of Eq. (9) we have the total time needed for the coagulation of k enclosures and on the right-hand side the total time needed for the coagulation of $(k + 1)$ enclosures. In the next section we describe the accurate computational implementation of the enclosure interaction.

After each time step we reconsider the total number of the particles in the system, or in other words the total volume represented in our simulation. If the total number of the particles is larger than our chosen certain critical number N_{crit} , then N_{comp} number of particles are randomly chosen to be our new system. Next we rescale the volume of the system by taking the ratio of the total volume of the particles in our new system to the total volume of the particles in the previous system with N_{crit} particles,

$$s = \frac{\sum_{i=1}^{N_{\text{comp}}} V_i}{\sum_{i=1}^{N_{\text{crit}}} V_i}, \tag{10}$$

determines the new volume represented in our simulation with N_{comp} particles

$$V_{\text{comp}} = sV_{\text{comp}}. \tag{11}$$

The revised V_{comp} is then used in the computation of the coagulation and nucleation (monomer generation) times.

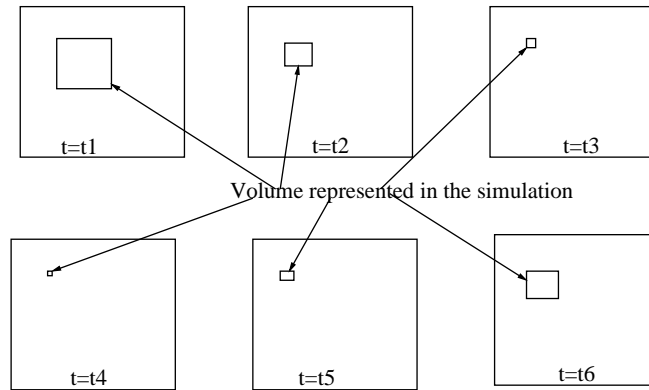


Fig. 3. Schematic description of hierarchical structure of MC at different increasing time instants, $t_1 < t_2 < \dots < t_6$.

On the other hand, if the total number of the droplets is less than certain n_{crit} we top up our system by replicating each particle with its equivalent enclosure state. In order to preserve the physical connection to real time, the topping up process must preserve the average behavior of the system corresponding to the time prior to topping up. In particular, one has to ensure that the characteristic time for droplet coagulation stays the same. In this case it is necessary to increase the system volume in proportion to the increase in droplets.

Because of the use of a time-dependent scaled simulation volume we call our approach hierarchical hybrid Monte-Carlo (Fig. 3)

4. Numerical implementation

To implement the numerical computation we define the coagulation probability by

$$p_{ij} = \frac{K_{ij}^F}{K_{\text{max}}^F}, \quad (12)$$

where K_{max}^F is the maximum value of the coagulation kernel among all droplets. This probability should in principle be normalized by the sum of K_{ij}^F , but the choice of K_{max}^F is often employed in order to increase the rate of acceptance. It also has the advantage of saving CPU time, because the computation of the sum of k_{ij} over all the enclosures is quite expensive.

A coagulation event is determined to occur only if a randomly drawn number from a uniform distribution is smaller than the probability of the coagulation p_{ij} . If the coagulation is rejected, two new particles are picked and the above steps are repeated until the coagulation condition is satisfied. On the completion of this step the time increment ΔT is computed according to (4).

At the same time the time increment for the nucleation of n_{nucl} particles is computed. For our numerical simulation we follow previous experimental and numerical studies on the vapor phase formation of iron oxide monomer (Biswas et al., 1997), and assume that the production of the particles will be given at time t by

$$N_{\text{nucl}} = N_0(1 - \exp(-kt)), \quad (13)$$

where N_{nucl} are the number of particles produced up to time t , N_0 are the total number of monomers and k , is the unimolecular rate constant for monomer production. For the exponential rate of production, the time interval for the production of n_{nucl} particles in a simulation volume V_{comp} is given by

$$\Delta t_n = \frac{V_{\text{comp}}}{V_0} \frac{n_{\text{nucl}}}{N_0 R} \exp(kt). \quad (14)$$

Based on the time increments Δt_n and ΔT we determine the computational time increment as $\Delta t_{\text{comp}} = \min(\Delta t_n, \Delta T)$.

If Δt_n is smaller than ΔT (the latter is the inter-event time for droplet coagulation) we nucleate n_{nucl} particles. Note that some portion of the nucleated particles (in our case 1/6, based on experimental conditions) are iron particles, and the rest ($5/6 n_{\text{nucl}}$) are silica particles. Further, we add Δt_{comp} to the time increment counted from the last droplet coagulation, Δt_{coag} ,

$$\Delta t_{\text{coag}} = \Delta t_{\text{coag}} + \Delta t_n. \quad (15)$$

If Δt_n is larger than ΔT , we set Δt_{coag} to zero, and perform particle coagulation based on the types of particles that were chosen. The following cases are possible: (a) If both particles are of the same type and homogeneous, then a new particle of the same type with volume $V_i + V_j$ is formed and the particles i and j are removed. (b) If the particles are homogeneous, but of different types; then the resulting particle is a droplet with volume $V_i + V_j$ with one enclosure whose volume corresponds to the volume of iron particles. (c) If one of the selected particles is homogeneous and the other is a heterogeneous particle. If a homogeneous particle is iron then the resulting particle is heterogeneous and its internal state as well as its volume change. The resulting particle will have one more enclosure and its volume will be $V_i + V_j$. If a homogeneous particle is silica then the resulting particle is heterogeneous and its internal state does not change, but its volume does. The volume of the resulting particle will be $V_i + V_j$. (d) If both particles are heterogeneous particles; then the resulting particle has volume $V_i + V_j$ and the enclosure distribution of the resulting droplet is the some of the enclosure distributions of the particles i and j .

Further, the enclosure interactions are handled in the following way. Based on elapsed time interval Δt_{comp} the enclosure interactions in each droplet are performed in the following way. After each l th successful enclosure collision in a droplet of volume V we compute the inter-event time for a collision,

$$\Delta t_l = \frac{2V}{\sum_{i=1}^{n-l} \sum_{j=1}^{n-l} K_{ij}^{\text{D}}}. \quad (16)$$

If this inter-event time is less than Δt_{comp} one performs additional collisions until the sum of the inter-event enclosure collision times is larger than Δt_{comp} . As soon as the sum of inter-event enclosure collision times becomes larger than Δt_{comp} one stops the enclosure coagulation and computes the extra time spent during the enclosure interactions. Assume there were k enclosure interactions with the inter-event times Δt_l ($l = 1, 2, \dots, k$). Then the extra time spent during the enclosure interactions is defined for each droplet and given by

$$\sum_{l=1}^k \Delta t_l - \Delta t_{\text{comp}}. \quad (17)$$

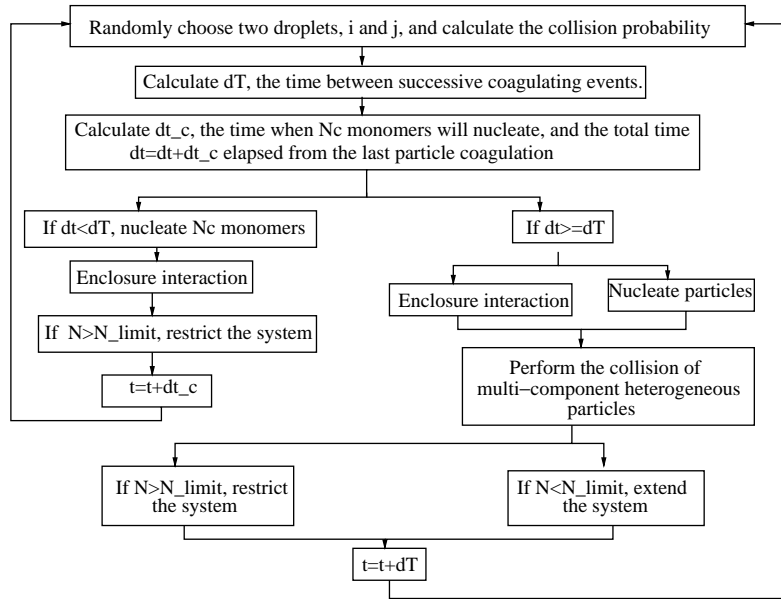


Fig. 4. Flow chart of the Monte-Carlo algorithm.

This extra time is taken into account at the next time step Δt_{comp} . In particular, first the enclosure coagulation at the next time step inside the droplet is increased by the amount of extra time. At the end of each times step the extra time spent during enclosure interactions is updated. We also would like to note that if two droplets collide then the extra time spent in the resulting droplet is taken to be the sum of the extra times spent in each droplet.

The enclosure interaction in a droplet is performed in the same way as for droplets. The probability of the collision of randomly selected two enclosures i and j is given by

$$p_{ij} = \frac{K_{ij}^D}{K_{\max}^D}, \quad (18)$$

where K_{\max}^D is the maximum value of the coagulation kernel among all droplets.

When the number of the droplets are below some threshold value we replicate the droplets and their internal state. When the number of particles are above some given threshold value $N_{\text{threshold}}$ we randomly choose N_{comp} particles and compute the new computational volume.

A flow chart of our Monte Carlo algorithm is depicted in Fig. 4.

5. Simulation results

The hierarchical hybrid MC approach is applied to the growth of $\text{SiO}_2/\text{Fe}_2\text{O}_3$ binary aerosol. The simulation begins with adding silica and iron monomers of size 0.5 nm with exponential rate k given by (13). The total volume ratio of the silica to the iron particles in the system is kept constant and equal to 5 at all times. We consider the total volume loading, $N_{\text{total}}V_{\text{monomer}}$, to be $1.6e - 7$.

Two temperature settings are considered, $T = 2400, 2600$ K. Since silica is the major phase, it is the working fluid whose viscosity will govern the rate of Brownian transport of the minor phase and therefore the growth rate of enclosures. The viscosity of the major component silica (SiO_2) as a function of temperature is given by (Jans, Lakshminarayanan, Lorentz, & Tomkins, 1968)

$$\mu = 10^{-8.6625(1-3556.03K/T)} \frac{\text{kg}}{\text{m s}}, \quad (19)$$

and the density of SiO_2 is held constant at $\rho = 5.5$ g/cc. The dimensional parts of collision kernels are given by

$$K^D = \frac{2kT}{3\mu},$$

$$K^F = \left(\frac{3}{4\pi}\right)^{1/2} \left(\frac{6kT}{\rho}\right)^{1/2} V_{\text{monomer}}^{1/6}. \quad (20)$$

Note that K^D is a very strong function of temperature, while K^F is essentially temperature independent.

Since an iron oxide and silica are not miscible, an accommodation factor, α , is used in heterogeneous condensation. Two values of α will be used in the numerical simulations, $\alpha = 1$ and 0.025. In the numerical simulations the monomer production rate is given by (13)

$$N_{\text{nucl}} = 4.16e - 9(1 - \exp(-kt)) \text{ mol/cc/s}, \quad (21)$$

with the variable rate constant k . In particular, we take k to be sensitive to temperature and given by $5.5e + 5 \exp(-5030/T)/\text{s}$ or $5.5e + 5 \exp(-10060/T)/\text{s}$.

The total number of the droplets in our numerical simulation is kept always above 1500. The critical number of particles when we truncate the system to 1500 droplets are taken to be 4500. Note that mean number of the enclosures per droplet can reach ~ 2000 . Thus, the total number of iron particles in the system is $2e + 6!$ To handle such large systems the code stores and deals with the droplets and their internal state in arrays. In particular, we store all the enclosures in an array, u_i , $i = 1, \dots, N$, where u_i is the volumes of the enclosures. Then we define the array for the number of the enclosures in each droplet, n_i , $i = 1, \dots, n$ and the array for the volume of each droplet V_i , $i = 1, \dots, n$, where V_i is the volume of the droplets. Here, n is the number of the droplets and N is the total number of the enclosures. After each coagulation process we sort all the enclosures, u_i and the droplets V_i .

Before discussing the simulation results we would like to make a comment about the use of mean-field equations (in our coagulation constants) for enclosures. One can argue that the description of the enclosures on statistical terms makes sense only if the number of enclosures is sufficiently large. This criticism can be resolved, however, since our system contains a large number of similar droplets. While the behavior of enclosures in a single droplet may not be well described statistically, the behavior of the enclosures in a large number of similar droplets can be described statistically. In that sense we consider the most likely behavior of enclosures in a droplet. We will show later that the behavior of enclosures in each droplet is similar and mean number of enclosures per droplet increases. Moreover, we would like to note that it would be easy to incorporate a particular dynamics associated with small number of particles in MC simulations.

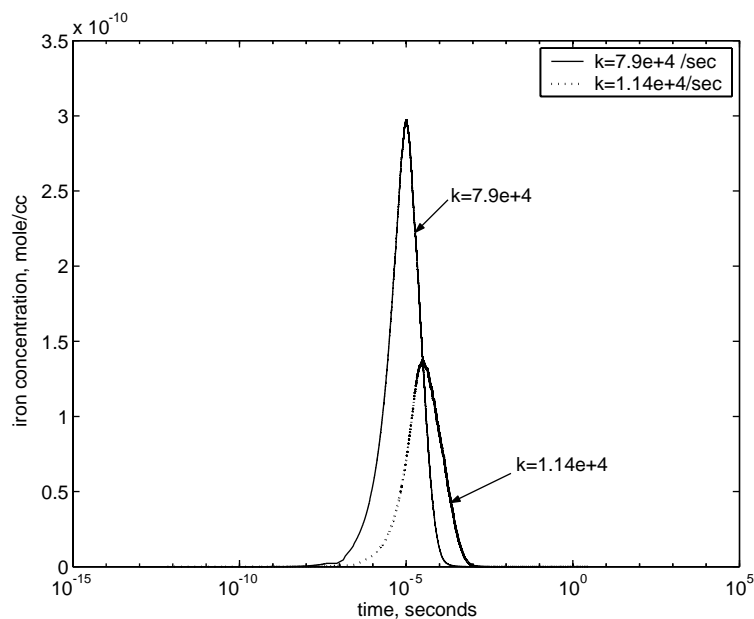


Fig. 5. Iron monomer concentration, $\alpha = 0.025$, $T = 2600$ K.

In our first numerical example (Fig. 5), we calculate the iron concentration for different monomer production rates. As expected a larger monomer production rate constant results in a more rapid appearance of the monomer, with a higher peak value.

The polymerization of iron monomer is insensitive to temperature because the dynamics of monomers is governed by free molecule coagulation which is a very weak function of temperature. Note that for the purposes of these calculations we neglect three-body energy transfer effects (Zachariah and Tsang, 1993, 1995). By contrast, the concentration of iron monomers are very sensitive to the sticking coefficient, α (Fig. 6). A small α results in a very large monomer pool. Indeed because of small sticking coefficient iron monomers would most likely coagulate with other iron particles. Since the concentration of iron monomers is five times less than that of silica, the probability of chosen two random particles to be iron monomers is very small. The presence of large iron monomer pool implies that heterogeneous growth processes for the minor phase is very important route to growth, particularly when one considers that the minor component is primarily interacting with an aerosols surface comprised primarily of the major phase.

Next we study the normalized variance of droplets (see Fig. 7). A larger rate of monomer production results in a smaller variance as homogeneous nucleation becomes a more dominant growth mode relative to heterogeneous condensation. Essentially, at the highest source rates the system has not had sufficient time to produce enough particulate surface area to compete for the monomer, which because of its higher concentration favors dimer formation (see Fig. 5). In addition to this effect, the smaller the production rate of monomer the longer the monomer production will last, thus we observe monomers as well as large particles, and the variance of droplet size distribution increases until the production of monomers ends. At large times, relative to monomer production, the value of the normalized variance clearly approaches an asymptotic value or self-preserving condition.

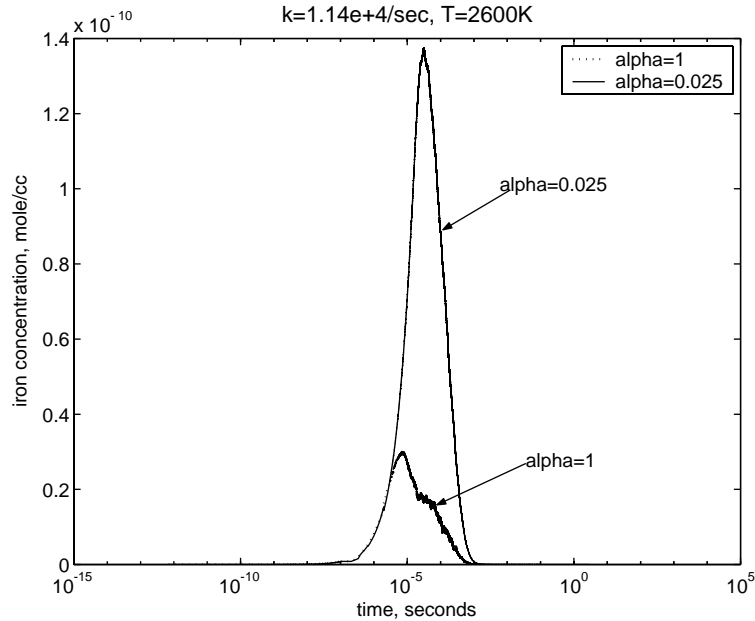


Fig. 6. Iron monomer concentration for different values of α . Monomer production rate, $k = 1.14e + 4/s$ (see (21)).

We now turn our attention in Fig. 8, to the effect of the sticking coefficient, α on the normalized variance of droplets. If α is small, then the monomer concentration remains high, and from the point of view of the size variance, the behavior is similar to having a low monomer production rate. The longer lasting monomer widens the size distribution and delays the onset of the self-preserving condition.

Thus, far we have focused our numerical simulations on the initial behavior of our multi-component system, which we conclude is very sensitive to the sticking coefficient. We turn our attention to the longer time behavior of the system. Here because the monomer has been exhausted the sticking coefficient has no role to play and we restrict our next numerical simulations to the case where $\alpha = 1$.

One of the quantities of interest is the phase segregation process which can be assessed by addressing the relative volume growth of enclosure due to the presence of the major phase. In Figs. 9 and 10 we plot the ratio of mean volume growth of droplets to enclosures, $\bar{V}_{\text{SiO}_2}/\bar{V}_{\text{Fe}_2\text{O}_3}$. This quantity is an indicator of the relative volume growth of iron oxide particles. Note that in the absence of the droplets, the enclosures would now be the aerosol and would coagulate in the free-molecular regime, and their growth rate would be proportional to the growth rate of droplets (note that the density of SiO_2 and Fe_2O_3 are very similar). More precisely, the growth rate of the enclosures (would now be the aerosol) is $1/c$ times the growth rate of the droplets (c represents the ratio of the volume fractions of silica to iron which is taken to be 0.2 in our simulations). Thus, $\bar{V}_{\text{SiO}_2}/\bar{V}_{\text{Fe}_2\text{O}_3}$ is an indicator of relative moderated growth rate of iron oxide due to the presence of the major phase. We see from Fig. 9 that introducing the major phase, SiO_2 , we effectively moderate the growth rate of the minor phase by some ~ 1500 times in 0.25 s. Comparing Figs. 9 and 10 we notice that a slight change in the temperature drastically increases the volume growth of enclosures.

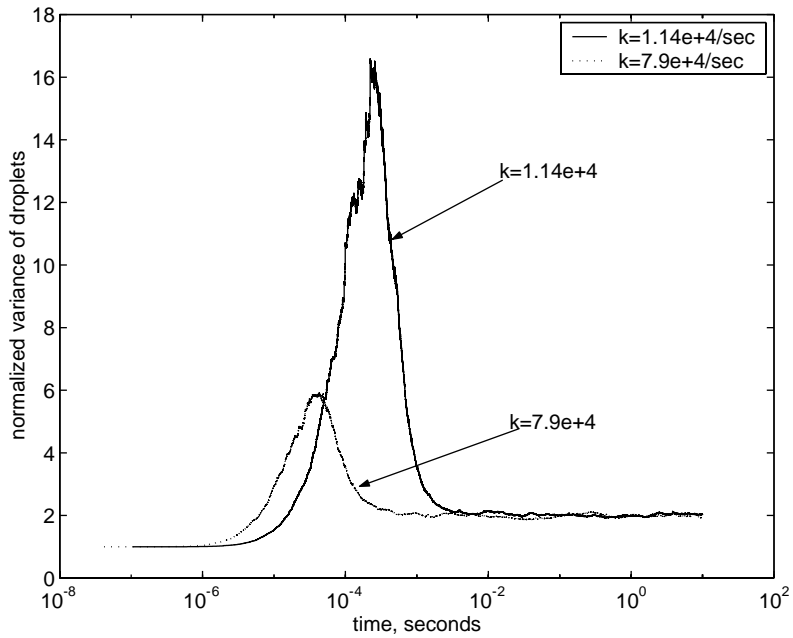


Fig. 7. Normalized variance of droplets for different kinetics: $\alpha = 1$, $T = 2600$ K.

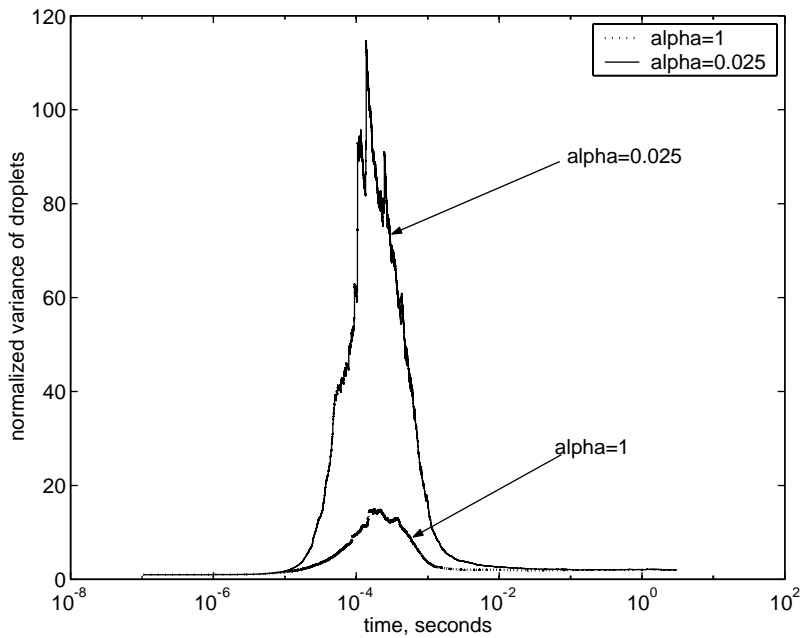


Fig. 8. Normalized variance of droplets for different values of α : $k = 1.14e + 4/s$, $T = 2600$ K.

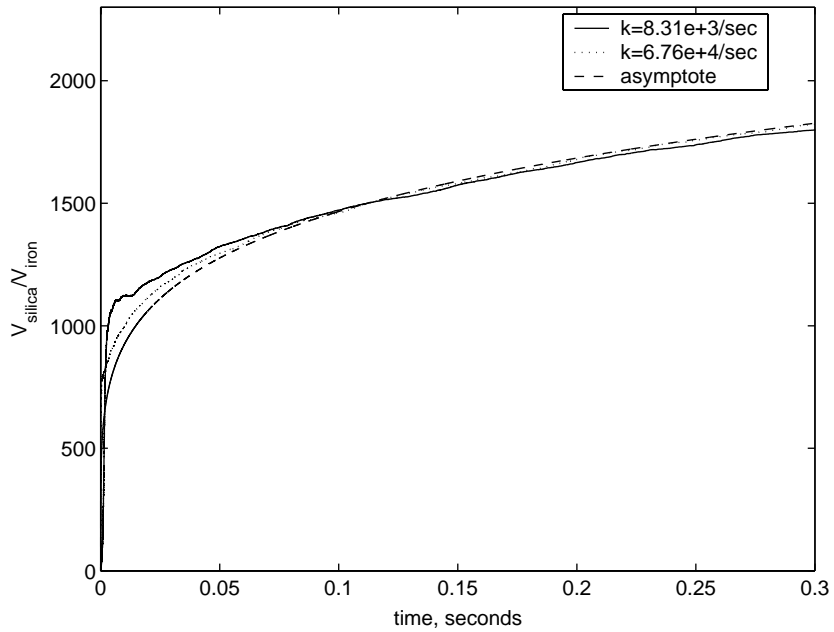


Fig. 9. Relative growth rate moderation for different k : $\alpha = 1$, $T = 2400$ K. The asymptote curve (designated by dashed line) grows $\sim t^{1/5}$, t is time.

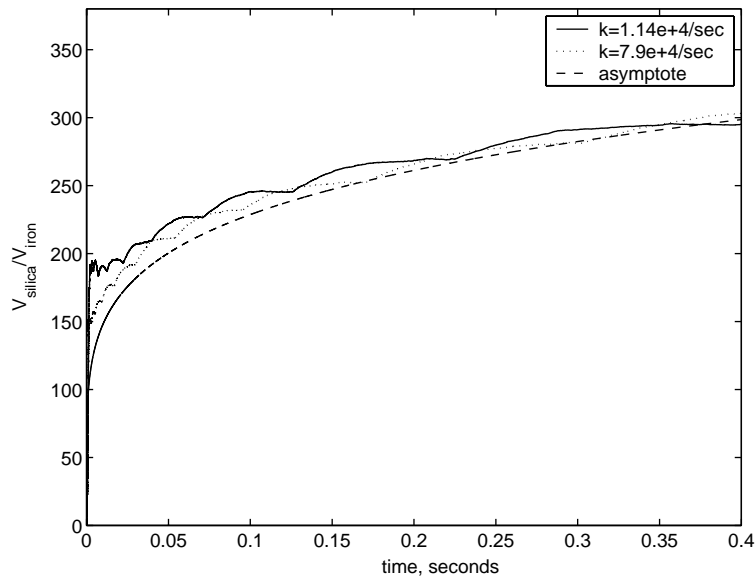


Fig. 10. Relative growth rate for different k : $\alpha = 1$, $T = 2600$ K. The asymptote curve (designated by dashed line) grows as $\sim t^{1/5}$, t is time.

Indeed, because of the lower viscosity of the major phase (silica droplet) the moderation rate will be significantly diminished, thus the coagulation of the enclosures will be faster, and therefore the enclosure average volume will be larger. More importantly perhaps is that the presence of the major phase can be used as a very significant moderator to nanoparticle growth with the temperature being the control variable (through the viscosity of the major phase).

We notice from Figs. 9 and 10 that if the monomer production rate is slower then the relative volume growth is higher at initial times. This can be explained in the following way. If the monomer production rate is slow then the particles have sufficient time to grow. During the growth the silica particles will grow faster than the iron particles because whenever iron particles become enclosures their growth is moderated. On the other hand, at higher rates, due to the excess of monomers that have not coagulated, the relative volume growth diminishes.

From Figs. 9 and 10 it is also clear that the relative volume growth increases at a slow rate at large times. In these figures we plot a curve (designated by the dashed line) showing the asymptotic behavior (large time) of the relative volume growth. The asymptotic behavior of the relative volume growth is obtained from the following scaling argument. Balancing the characteristic times for enclosure and droplet coagulations, we obtain

$$\frac{1}{K_0^F N} \sim \frac{\bar{V}}{K^D \bar{n}}, \quad (22)$$

where \bar{V} is mean droplet volume, \bar{n} is mean number of enclosures per droplet, and $K_0^F = K^F (\bar{V}/V_{\text{monomer}})^{1/6}$. Further taking the volume fraction of the enclosures in each droplet with volume V to be cV (c is the total volume fraction of iron to silica which is assumed to be constant at all times), (22) becomes

$$\frac{\bar{V}}{K_0^F N \bar{V}} \sim \frac{\bar{u}}{cK^D}, \quad (23)$$

where \bar{V} is the mean volume of droplets, and \bar{u} is the mean volume of the enclosures. From this expression

$$\frac{\bar{V}}{\bar{u}} \sim \frac{K_0^F \phi}{cK^D}, \quad (24)$$

where ϕ is the volume fraction of droplets. Next we note that K_0^F grows as $\bar{V}^{1/6}$, while the Brownian kernel is independent of the mean volume growth. Assuming that droplet size distribution is self-preserving at large times, then $\bar{V}^{1/6}$ would grow as $t^{1/5}$ (Friedlander, 2000). Thus \bar{V}/\bar{u} would grow as $t^{1/5}$. The asymptote curves (designated by dashed lines) in Figs. 9 and 10 are of the form $x \sim t^{1/5}$. Clearly, at large times the growth of the relative volume has the behavior $\sim t^{1/5}$.

In our analytical calculations of relative growth we assumed that the volume fraction of the enclosures in a droplet of volume V is given by cV . To show this, in Fig. 11 we calculate the normalized variance of volume fraction of the enclosures in a droplet. Since the ratio of the total volumes of SiO_2 and Fe_2O_3 is constant at all times the mean value of enclosure volume fractions is c . As we see from our numerical results that enclosure volume fractions are almost uniform at large times, i.e., the normalized variance reaches to unity. Moreover, for smaller rates the normalized variance approaches to unity faster, because the production of monomers terminates earlier.

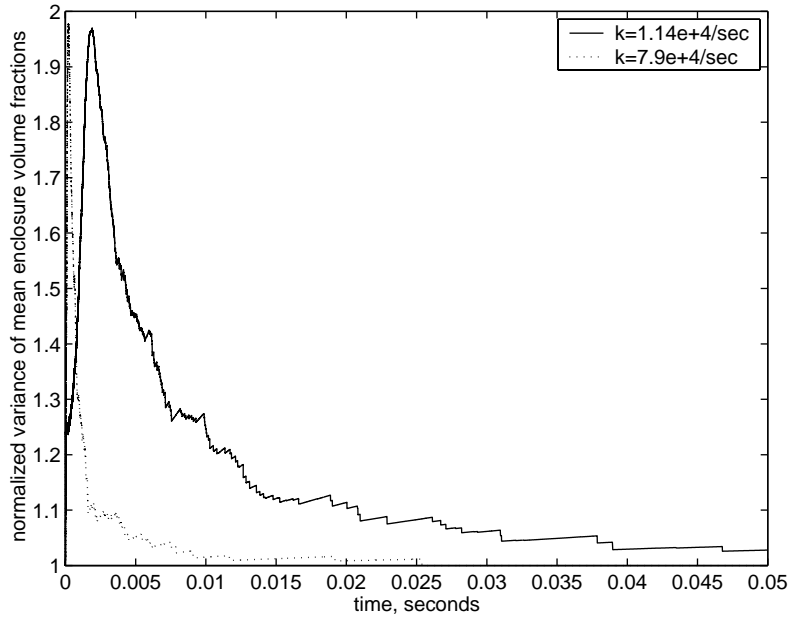


Fig. 11. Normalized variance of enclosure volume fraction of each droplet for different k : $\alpha = 1$, $T = 2400$ K.

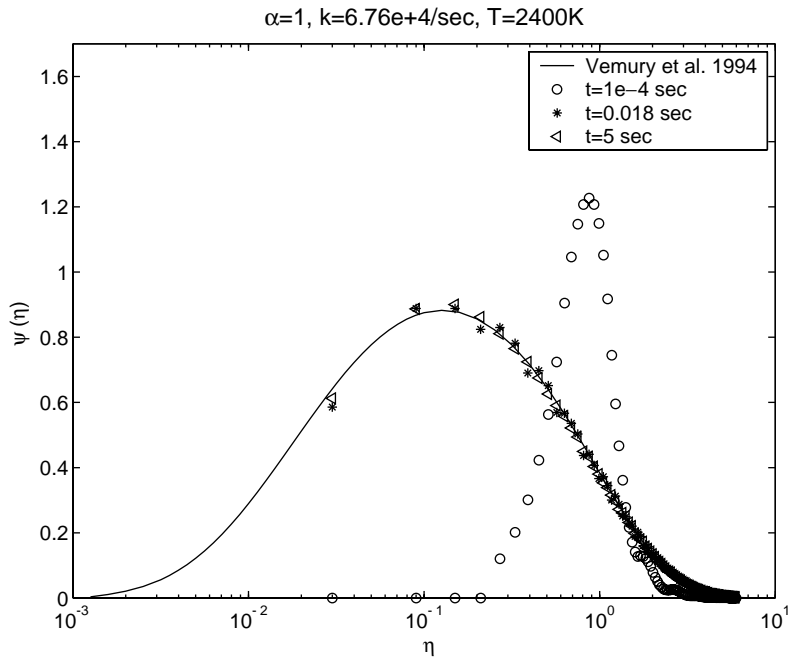


Fig. 12. The enclosure size distribution at $T = 2300$ K. Dimensionless number density, $\psi(\eta) = n(v, t)\bar{v}/n^\infty$ versus dimensionless volume, $\eta = v/\bar{v}$. The numerical values of the self-preserving distribution for the Brownian regime (solid line) is taken from Vemury et al. (1994).

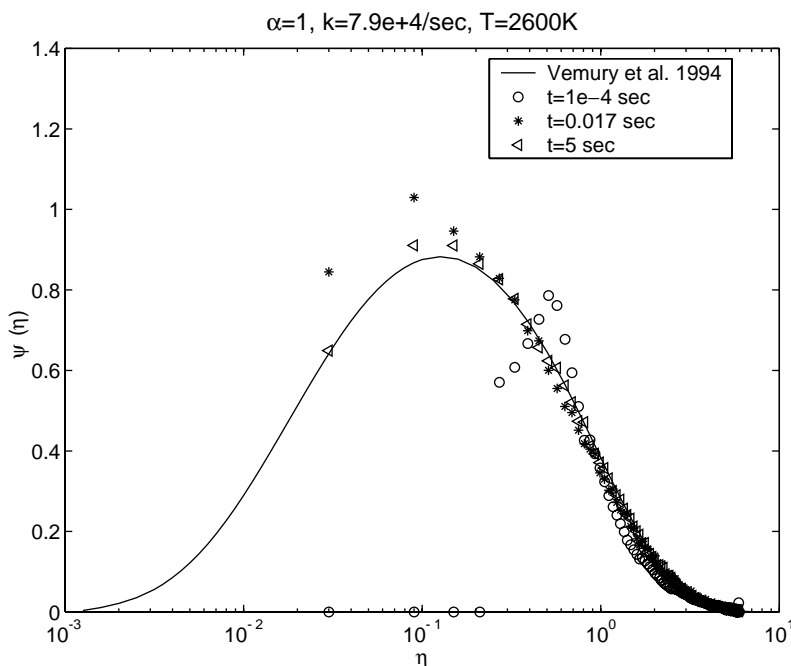


Fig. 13. The enclosure size distribution at $T = 2300$ K. Dimensionless number density, $\psi(\eta) = n(v, t)\bar{v}/n^\infty$ versus dimensionless volume, $\eta = v/\bar{v}$. The numerical values of the self-preserving distribution for the Brownian regime (solid line) is taken from Vemury et al. (1994).

Finally, in the last two figures (Figs. 12 and 13) we present the enclosure distribution at different times by plotting the dimensionless enclosure size distribution $\psi(\eta) = n(v, t)\bar{v}/n^\infty$, versus the dimensionless volume $\eta = v/\bar{v}$, where n^∞ is the total number of enclosures. Clearly, the distributions have approached to a self-preserving form for Brownian coagulation (the numerical values of $\psi(\eta)$ are taken from Vemury, Kusters, and Pratsinis (1994)). This is associated with the fact that at large times the mean number of enclosures per droplet is large. The mean number of enclosure per droplet can be calculated from (22), $\bar{n} = c\bar{V}/\bar{u}$. If mean number of the enclosures per droplet is large enough, the self-preserving form of the enclosure distribution is approximately the same as that corresponding to the Brownian coagulation, and the coagulation of the droplets does not influence the enclosure size distribution (see Efendiev & Zachariah, 2002).

Note that if the number of enclosures in a droplet becomes too large for the simulation, one can truncate the enclosure system within a droplet by randomly picking a certain number of enclosures and adjusting the corresponding computational volume (similar to the droplets). Observing that when the mean number of enclosures per droplet is large, the enclosure population reaches the self-preserving form corresponding to Brownian coagulation, it is unnecessary to run the simulations further.

6. Conclusions

In this paper we have presented a hierarchical hybrid Monte Carlo technique to simulate the simultaneous nucleation, coagulation and phase segregation of immiscible two-component aerosols.

Our approach combines two MC simulations with numerical treatment of a kinetic nucleation process. One MC loop simulates the coagulation of droplets and the other simulates the interaction between enclosures. To account for nucleation we introduce the hierarchy of computational volumes represented in the simulation. The method was applied to the $\text{SiO}_2/\text{Fe}_2\text{O}_3$, binary system which we have studied in our previous work (Struchtrup et al., 2001; Efendiev et al., 2002) using the sectional models.

Our MC approach allows us to compute various average properties of our system an initial as well as at large times. The initial time behavior depends on the parameters of nucleation, and sticking factors, while the asymptotic behavior is essentially independent of the initial conditions, but very sensitive to temperature.

The relative volume growth of the enclosures due to the presence of droplets is computed. The computations show that this quantity increases at a slow rate and that the asymptotic behavior is independent of the initial conditions with the exception of temperature. The computations of the statistics of enclosure size distribution indicate that the enclosure size distribution reaches the self-preserving condition at large times and is very close to the self-preserving distribution for Brownian coagulation.

One of the main advantages of our MC approach over the sectional multi-variate models is that MC framework introduced here is amenable to the inclusion of additional phenomena.

References

- Biswas, P., Wu, C., Zachariah, M. R., & McMillen, B. K. (1997). Vapor phase growth of iron oxide-silica nanocomposite. Part II: Comparison of a discrete-sectional model predictions to experimental data. *Journal of Materials Research*, 12, 714.
- Biswas, P., Yang, G., & Zachariah, M. R. (1998). In situ processing of ferroelectric materials from lead streams by injection of gas-phase titanium precursors. *Combustion Science and Technology*, 134, 183.
- Biswas, P., & Zachariah, M. R. (1997). In situ immobilization of lead species in combustion environments by injection of gas phase silica sorbent precursors. *Environmental Science and Technology*, 31, 2455.
- Efendiev, Y., Luskin, M., Struchtrup, H., & Zachariah, M. R. (2002). A hybrid sectional-moment model for coagulation and phase segregation in binary liquid nanodroplets. *Journal of Nanoparticle Research*, 4, 61.
- Efendiev, Y., & Zachariah, M. R. (2001). A model for two-component aerosol coagulation and phase separation: A method for changing the growth rate of nanoparticles. *Chemical Engineering Science*, 56, 5763.
- Efendiev, Y., & Zachariah, M. R. (2002). Hybrid Monte-Carlo method for simulation of two-component aerosol coagulation and phase segregation. *Journal of Colloid and Interface Science*, 249, 30.
- Ehrman, S., Friedlander, S. K., & Zachariah, M. R. (1998). Characterization of $\text{SiO}_2/\text{TiO}_2$ nanocomposite aerosol in a premixed flame. *Journal of Aerosol Science*, 29, 687.
- Ehrman, S., Aquino-Class, M., & Zachariah, M. R. (1999a). Effect of temperature and vapor-phase encapsulation on particle growth and morphology. *Journal of Materials Research*, 14, 1664–1671.
- Ehrman, S., Friedlander, S. K., & Zachariah, M. R. (1999b). Phase segregation in binary $\text{SiO}_2/\text{TiO}_2$, $\text{SiO}_2/\text{Fe}_2\text{O}_3$ aerosols formed in a premixed flame. *Journal of Materials Research*, 14, 4551.
- Friedlander, S. K. (2000). *Smoke, dust and haze*, 2nd Ed. Oxford University Press.
- Gillespie, D. (1975). An exact method for numerically simulating the stochastic coalescence process in cloud. *Journal of Atmospheric Science*, 32, 1977–1989.
- Jans, G., Lakshminarayanan, F. D. G., Lorentz, P., & Tomkins, R. (1968). Molten salts: Vol. 1, electrical conductance, density, and viscosity data. US National Standard Reference Data Series, US National Bureau of Standards, Washington.
- Liffman, K. (1992). A direct simulation Monte-Carlo method for cluster coagulation. *Journal of Computational Physics*, 100, 116–127.

- McMillin, B. K., Biswas, P., & Zachariah, M. R. (1996). In situ characterization of vapor phase growth of iron oxide–silica nanocomposite. Part I: 2-d planar laser-induced fluorescence and mie imaging. *Journal of Materials Research*, *11*, 1552–1561.
- Rosner, D., & Yu, S. (2001). Monte Carlo simulation of aerosol aggregation and simultaneous spheroidization. *A.I.Ch.E.*, *47*, 545–561.
- Scott, W. (1967). Poisson statistics in distributions of coalescing droplets. *Journal of Atmospheric Science*, *24*, 221.
- Shah, B., Ramakrishna, D., & Borwanker, J. (1977). Simulation of particulate systems using the concept of the interval of quiescence. *A.I.Ch.E.*, *23*, 897–904.
- Smith, M., & Matsoukas, T. (1998). Constant-number Monte Carlo simulation of population balances. *Chemical Engineering Science*, *53*, 1777–1786.
- Struchtrup, H., Luskin, M., & Zachariah, M. R. (2001). A model for kinetically controlled internal phase segregation during aerosol coagulation. *Journal of Aerosol Science*, to appear.
- Tandon, P., & Rosner, D. (1999). Monte Carlo simulation of particle aggregation and simultaneous restructuring. *Journal of Colloid and Interface Science*, *213*, 273–276.
- Vemury, S., Kusters, K., & Pratsinis, S. (1994). Time-lag for attainment of the self-preserving particle size distribution by coagulation. *Journal of Colloid and Interface Science*, *165*, 53–59.
- Zachariah, M. R., Aquino-Class, M., Shull, R., & Steel, E. (1995). Formation of super-paramagnetic nanocomposite from vapor phase condensation in a flame. *Nanostructured Materials*, *5*, 383.
- Zachariah, M. R., Shull, R., McMillin, B. K., & Biswas, P. (1996). In situ characterization and modeling of the vapor phase growth of a supermagnetic nanocomposite. *Nanotechnology*, *622*, 42–63.
- Zachariah, M. R., & Tsang, W. (1993). Application of ab-initio molecular orbital and reaction rate theories to nucleation kinetics. *Aerosol Science Technology*, *19*, 499.
- Zachariah, M. R., & Tsang, W. (1995). Theoretical computation of thermochemistry, energetics and kinetics for high temperature $\text{Si}_x\text{H}_y\text{O}_z$ reactions. *Journal of Physical Chemistry*, *99*, 5308.